Vibrational Spectrum of a Picosecond Intermediate in the Artificial BR5.12 Photoreaction: Picosecond Time-Resolved CARS of T5.12

L. Ujj,[†] Yidong Zhou,[†] M. Sheves,[‡] M. Ottolenghi,[§] S. Ruhman,[§] and G. H. Atkinson*,[†]

Contribution from the Department of Chemistry and Optical Science Center, University of Arizona, Tucson, Arizona 85721, Department of Chemistry, Weizmann Institute, Rehovet, Israel, and Department of Chemistry, Hebrew University, Jerusalem, Israel

Received May 3, 1999. Revised Manuscript Received August 30, 1999

Abstract: The vibrational spectrum of an intermediate, T5.12, in the photoreaction of an artificial bacteriorhodopsin (BR) pigment containing a five-membered carbon ring spanning the $C_{12}-C_{13}=C_{14}$ bonds (BR5.12) is measured by picosecond time-resolved coherent anti-Stokes Raman spectroscopy (PTR/CARS). Observed initially by picosecond transient absorption (PTA) measurements, T5.12 is the only intermediate in the BR5.12 photoreaction (i.e., T5.12 decays only to BR5.12). BR5.12 does not have a photocycle analogous to that in native BR, presumably because the five-membered ring blocks the reaction coordinate leading to $C_{13}=C_{14}$ bond isomerization. Since T5.12 may therefore represent the molecular events (reaction coordinates) that precede $C_{13}=C_{14}$ bond isomerization, its vibrational spectrum may aid in elucidating the **primary** reaction coordinate-(s) in the BR photocycle. Although T5.12 is identified via a red-shifted absorption (660 nm maximum, <3 ps formation with 3 ps BR5.12 excitation and decay in 17 ± 1 ps), no spectroscopic data which directly characterize the retinal structure in T5.12, and thereby the role of bonding changes, have been available. The PTR/CARS vibrational data presented here show that T5.12 contains (i) an *all-trans* retinal configuration, (ii) significant hydrogen out-of-plane motion localized in specific normal modes, (iii) increased π-electron density in the C=C stretching modes manifested by frequency increases, (iv) restricted in-plane $C-CH_3$ rocking motion, and (v) a Schiff-base environment similar to that in BR5.12. These PTR/CARS data also confirm that T5.12 decays exclusively to BR5.12. The vibrational spectrum of T5.12 makes it evident that no complete C=C isomerization nor C−C rotation in any retinal bond occurs upon excitation of BR5.12. The excellent agreement between the kinetic lifetime of T5.12 (from PTA and PTR/CARS data) and its stimulated emission lifetime suggests that T5.12 may be an excited electronic state. In such a case, the PTR/CARS data presented here are the first to be reported from an excited electronic state of a protein. Regardless of whether T5.12 is an excited or ground electronic state, the vibrational spectra of T5.12 reflect the retinal structure(s) that **precedes** $C_{13}=C_{14}$ bond isomerization in the BR photocycle. The relevance of T5.12 PTR/CARS data to the native BR photocycle is discussed in terms of the intermediates K-590, J-625, and I-460. Direct analyses of the respective vibrational spectra of T5.12 and K-590 demonstrate that they contain distinctly different retinal structures, but since no vibrational data assignable directly to either I-460 or J-625 have been reported, comparisons of T5.12 with these intermediates are based only on analogy. Comparisons of the vibrational spectra of T5.12 and native BR intermediates independently provide insight into the structural changes in retinal that could occur prior to $C_{13}=C_{14}$ bond isomerization in native BR.

Introduction

Since the primary role played by $C_{13}=C_{14}$ bond isomerization in the room-temperature bacteriorhodopsin (BR) photocycle has long been recognized (for reviews see refs 1−3), essentially all mechanistic models proposed for energy storage/transduction in the BR photocycle have incorporated $C_{13}=C_{14}$ bond isomerization as the fundamental molecular step (i.e., primary reaction coordinate).[4−7] A central question remaining in all of these mechanisms, however, is at what point in the BR photocycle does $C_{13}=C_{14}$ bond isomerization occur. Uniformly, these models incorporate $C_{13}=C_{14}$ bond isomerization prior to the appearance of J-625 (i.e., proposing that J-625 has a 13-*cis* retinal) even though no spectroscopic data fully characterizing the structural degrees of freedom in J-625 have been reported. The vibrational spectrum of the K-590 intermediate formed upon the 3.5-ps decay of J-625 has shown that it contains a 13-*cis* retinal.[8,9] By placing $C_{13}=C_{14}$ isomerization prior to the ∼200-fs formation of J-625, these mechanisms have focused much attention on identifying the molecular properties associated with such a large structural transformation as isomerization over a <200-fs time scale.[10] This issue can be addressed experimentally by determining whether the retinal structure J-625 is 13-*cis* or

[†] University of Arizona.
[‡] Weizmann Institute.
[§] Hebrew University.

(1) Lanyi, J. K. *Nature* **1995**, *375*, 461−463.
(2) Maeda, A. *Isr. J. Chem.* **1995**, *35*, 387−400.
(3) Stoeckenius, W. *Protein Sci.* **1999**, *8*, 447−459.
(4) Schulten, K.; Tavan, P. *Nature* **1978**, *272*, 85−86.
(5) Fodor, S. P. A.; Ames, J. B.; Gebhard, R.; van den Berg, E. M. M.; Stoeckenius, W.; Lugtenburg, J.; Mathies, R. A. *Biochemistry* **1988**, *27*, 7097−7101.
(6) Dencher, N. A.; Dresselhaus, D.; Zaccai, G.; Büldt, G. *Proc. Natl. Acad. Sci. U.S.A.* **1989**, *86*, 7876−7879.
(7) Haupts, U.; Tittor, J.; Bamberg, E.; Oesterhelt, D. *Biochemistry* **1997**, *36*, 2−7.
(8) Brack, T. L.; Atkinson, G. H. *J. Mol. Struct.* **1989**, 289−303.
(9) Ujj, L.; Jäger, F.; Popp, A.; Atkinson, G. H. *Chem. Phys.* **1996**, *212*, 421−436.

10.1021/ja991447e CCC: $19.00
Published on Web 12/21/1999

all-trans. Unfortunately, the 3.5-ps lifetime of J-625 makes a determination of its vibrational degrees of freedom experimentally challenging.

Since the presence of intermediates and the kinetic parameters comprising the earliest stages of the BR photocycle have been determined almost exclusively by femto (FTA) and picosecond (PTA) absorption measurements, little, if any, direct spectroscopic information on retinal structural changes that comprise the I-460 to J-625 to K-590 transformations is available. The earliest room-temperature BR intermediate for which direct structurally sensitive measurements are available is K-590. These K-590 data are derived from room-temperature, time-resolved Raman (both picosecond time-resolved resonance (spontaneous) Raman (PTR[3])[8] and picosecond time-resolved coherent anti-Stokes Raman spectroscopy (PTR/CARS)[9]) and time-resolved infrared absorption[11] measurements. Time-resolved vibrational data of this type provide both structural and kinetic data simultaneously. In general, the kinetics derived independently from transient absorption and time-resolved vibrational spectroscopy are in excellent agreement. Structurally, these vibrational spectra (PTR/CARS) demonstrate that the retinal in K-590 has a twisted, 13-*cis* configuration over the 10 ps to 10 ns interval which relaxes into a more planar 13-*cis* retinal via changes in the hydrogen out-of-plane (HOOP) modes as a precursor to the L-550 intermediate.[12,13] Thus, it is known that C_{13}═C_{14} bond isomerization occurs no later than the formation of K-590.

The intermediates I-460 (<50-fs rise and <200−500-fs decay times[14−16]) and J-625 (<500-fs rise and 3.5-ps decay times (reviewed in ref 17)) have been originally identified respectively from the blue- (460 nm) and red-shifted (625 nm) absorption maxima observed in FTA or PTA data. Subsequent FTA data also attributed red-shifted absorption to I-460.[18,19] Specifically, absorption and stimulated emission signals have been assigned to I-460 respectively at 460 and 860 nm.[18,19] Based on comparisons between stimulated and spontaneous emission data,[18,19] it has been suggested that I-460 has an additional absorption band between 620 and 820 nm. This band is not observed directly in pump−probe experiments due to the masking effect of the strong fluorescence band appearing in the same region. Although both FTA[16,20] and PTA[21] data confirm the existence of J-625, somewhat different kinetic constants have been reported.[16,20,21] Neither I-460 nor J-625 has been stabilized at low temperature nor have their vibrational degrees of freedom been directly measured at room temperature. The duration of the laser pulses required to generate vibrational data from I-460 and J-625, as dictated by their respective <200−500-fs and 3.5-ps lifetimes, is so short that little of the information on the vibrational degrees of freedom needed to determine structural properties can be extracted from the large bandwidths of the resultant vibrational features. For example, even the 2-ps pulse width excitation required to obtain temporally separated vibrational data (e.g., Raman scattering) from J-625 produces vibrational bands with ∼7-cm^{-1} bandwidths. Even in the absence of structurally sensitive data, mechanistic models for the room-temperature BR photocycle attributing specific structures to both I-460 and J-625 are proposed, especially with respect to C_{13}═C_{14} bond isomerization, twisting, and/or distortion.[16,22]

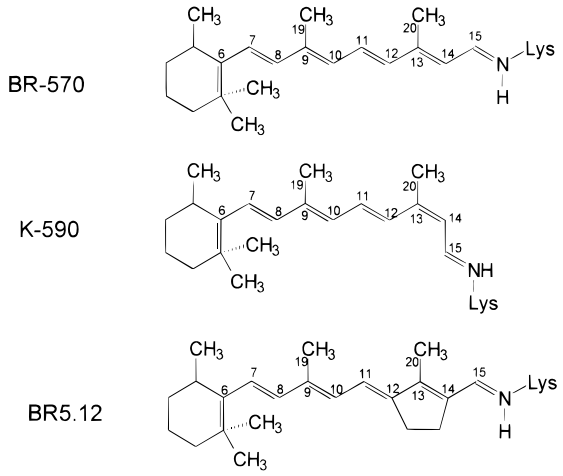

Figure 1. Retinal structures of (A) the *all-trans* retinal appearing in native BR-570, (B) the 13-*cis* retinal appearing in the native intermediate, K-590, and (C) the chemically modified retinal having a cyclopentene ring spanning the C_{12}−C_{13}═C_{14} bond region of the polyene chain appearing in BR5.12.

The photoreaction of the artificial BR pigment, BR5.12, containing a five-membered carbon ring spanning the C_{12}−C_{13}═C_{14} bond region in the retinal (Figure 1) offers an opportunity to address some of these issues experimentally. Although BR5.12 does not have a photocycle (the five-membered ring prevents the C_{13}═C_{14} bond isomerization), an intermediate, T5.12, is observed via PTA[23] that decays only to the stable ground state, BR5.12. In the work presented here, experimental advantage is taken of the relatively long (17 ± 1)-ps lifetime and red-shifted (660 nm) absorption of T5.12 to measure its vibrational spectrum via PTR/CARS. The vibrational spectrum of the stable BR5.12 itself also is measured via picosecond resonance CARS (PR/CARS) under experimental conditions that permit a direct comparison with the PTR/CARS T5.12 spectrum. Vibrational mode assignments of these PR/CARS and PTR/CARS data show that T5.12 is structurally distinct from BR5.12 and that T5.12 contains a retinal which is primarily *all-trans*. Relative to BR5.12, T5.12 (i) strengthens the C═C bond (increased bond order), (ii) significantly restricts in-plane C−CH_3 rocking motion, (iii) acquires a moderate degree of C−H out-of-plane motion, and (iv) maintains a Schiff-base bonding environment that is similar to that in BR5.12.

The structural changes occurring in the BR5.12 retinal are by themselves important given the general use of such artificial

(10) Ben-Nun, M.; Molnar, F.; Lu, H.; Phillips, J. C.; Martinez, T. J.; Schulten, K. *Faraday Discuss* **1998**, *110*, 447−462.
(11) Diller, R. *Chem. Phys. Lett.* **1998**, *295*, 47−55.
(12) Lohrmann, R.; Stockburger, M. *J. Raman. Spectrosc.* **1992**, *23*, 575−583.
(13) Weidlich, O.; Ujj, L.; Jäger, F.; Atkinson, G. H. *Biophys. J.* **1997**, *72*, 2329−2341.
(14) Nuss, M. C.; Zinth, W.; Kaiser, W.; Kolling, E.; Oesterhelt, D. *Chem. Phys. Lett.* **1985**, *117*, 1−7.
(15) Zhong, Q.; Ruhman, S.; Ottolenghi, M.; Sheves, M.; Friedman, N.; Atkinson, G. H.; Delaney, J. K. *J. Am. Chem. Soc.* **1996,** *118*, 12828−12829.
(16) Ye, T. Q.; Friedman, N.; Atkinson, G. H.; Sheves, M.; Ottolenghi, M.; Ruhman, S. *J. Phys. Chem.* **1999**, *103*, 5122−5130.
(17) Kochendoerfer, G. G.; Mathies, R. A. *Isr. J. Chem.* **1995**, *35*, 211−226.
(18) Gai, F.; McDonald, J. C.; Anfinrud, P. A. *J. Am. Chem. Soc.* **1997**, *119*, 6201−6202.
(19) Hasson, K. C.; Gai, F.; Anfinrud, P. A. *Proc. Natl. Acad. Sci. U.S.A.* **1996**, *93*, 15124−15129.
(20) Kandori, H.; Yoshihara, K.; Tomioka, H.; Sasabe, H.; Shichida, Y. *Chem. Phys. Lett.* **1993**, *211*, 385−391.
(21) Blanchard, D.; Gilmore, D. A.; Brack, T. L.; Lemaire, H.; Hughes, D.; Atkinson, G. H. *Chem. Phys.* **1991**, *156*, 155−170.
(22) Dexheimer, S. L.; Wang, Q.; Peteanu, L. A.; Pollard, W. T.; Mathies, R. A.; Shank, C. V. *Chem. Phys. Lett.* **1992**, *188*, 61−66.
(23) Delaney, J. K.; Brack, T. L.; Atkinson, G. H.; Ottolenghi, M.; Steinberg, G.; Sheves, M. *Proc. Natl. Acad. Sci. U.S.A.* **1995**, *92*, 2101−2105.

BR pigments as models for the native BR photocycle. The vibrational spectrum of T5.12 reflects the degree to which the retinal structure can be altered when it contains a relatively rigid ring that effectively blocks C_{13}=C_{14} bond isomerization. Thus, T5.12 may represent the retinal structure that precedes C_{13}=C_{14} isomerization and, as such, provides insight into the primary reaction coordinate(s) in the native BR photocycle. The structure/function relationship between C_{13}=C_{14} bond isomerization and proton pumping in BR has been examined through studies of artificial BR pigments containing a variety of structural modifications, including the incorporation of various size carbon rings spanning different parts of the retinal chromophore.[24] Whenever motion around the C_{13}=C_{14} bond is sufficiently restricted to prevent permanent C_{13}=C_{14} bond isomerization, the proton pumping function of BR fails to materialize.[23] Thus, mechanistically, the absence of proton pumping is directly correlated with the absence of a *cis* C_{13}=C_{14} bond (i.e., K-like intermediate, but not necessarily a J-like species).

PTR/CARS vibrational data from T5.12 also indirectly provide insight into the respective structures of the native BR intermediates. For example, comparisons of vibrational spectra assignable to T5.12 and K-590 (PTR/CARS data) demonstrate that these two intermediates contain completely different retinal structures, *vide infra*. No comparable vibrational data for either I-460 or J-625 have yet been reported, and therefore information pertinent to I-460 or J-625 can be obtained only via analogies involving their respective kinetics and absorption spectroscopy. The red-shifted (relative to its ground state) absorption spectra of T5.12 and J-625, together with their respective formation (50 fs[16] vs ~500 fs[16]) and decay (17 ps [23] vs 3.5 ps[21]) times suggest that they may have similar functions in their respective photoreactions. The absorption spectra and emission properties of I-460 and T5.12 also have some similarities. Both absorb over a broad (e.g., 460−820 nm) spectral region (suggesting an I5.12 designation) although their decays times are more than an order of magnitude different (17 ps vs <200−500 fs). Both also have stimulated emission signal near 860−900 nm suggesting that both are excited electronic state species. These comparisons, however, do not address the central issue of determining their respective retinal structures. Thus, in the absence of vibrational spectra assignable to I-460 and/or J-625, it remains reasonable to consider both intermediates as potentially analogous to T5.12. Experimentally, the longer lifetime of T5.12 makes it easier to record its vibrational spectrum than to record the vibrational spectrum of either I-460 or J-625.

Experimental Methods and Instrumentation

BR5.12 samples are obtained from a cell line of *halobacterium salinarium* and are purified according to established procedures.[23,25] The ratio between the absorbance of the BR5.12 sample at 280 nm and the absorbance at 570 nm of the light-adapted, purple membrane sample is ≈1.5. To isolate bacterio-opsin via the removal of *all-trans* retinal, BR5.12 is bleached for 24 h by focusing the output from a 500-W projector lamp through a 450-nm cutoff filter and a 5-cm path length infrared filter (liquid water) into a native BR solution containing 1 M NH_3OHCl, 1 M NaOH, and 1 M NaCl buffered at pH 7.0. After bleaching is completed, a 10 mM K_2HPO_4 buffer and a 3% w/v solution of bovine serum albumin (BSA) are added to eliminate the hydroxylamine and any excess *all-trans* retinal. The resultant sample is centrifuged three times.

The chemically modified retinal 5.12[23] (see Figure 1) is dissolved in ethanol (2% of the total volume of buffered opsin solution with a 1:1 molar ratio of opsin to retinal). The reconstitution of bacterio-opsin with the artificial retinal 5.12 occurs in the dark at room temperature over a 5-day period. The reconstituted BR5.12 sample is centrifuged to obtain a pellet that is resuspended in 10 mM K_2HPO_4 buffer to yield approximately 10 mL of a 2 OD sample in H_2O.

The instrumentation and experimental procedures used to record PTR/CARS signals are discussed in detail elsewhere,[26] and therefore only a brief description of the fundamental issues is presented here. The 1053-nm output (30-ps pulses at 76 MHZ repetition rate) of a cw, mode-locked Nd:YLF laser (Coherent, Antares 76) is used to generate second harmonic radiation from LBO (527 nm) crystal. The 527-nm radiation is used to pump three, independently controlled dye lasers (Coherent, model 701-3). Each dye laser is equipped with a cavity dumper (Coherent, models 7210 and 7220), three of which are synchronized to the mode locker of the Nd:YLF pump laser. The entire laser system is operated at a 400-kHz repetition rate to match the flow properties of the liquid sample jet. The velocity of the BR5.12 sample in the 400-μm square nozzle is adjusted to 12 m/s (laminar flow) to ensure a complete replacement of the sample volume (20 μm diameter) between the arrival of sets of laser pulses.

PTR/CARS signals are generated simultaneously from two separate sample compartments, reference and BR5.12.[26] This sample configuration minimizes long-term intensity drift and spectral shape changes associated with the lasers pulses. The reference compartment is a capillary containing a static water sample placed next to the glass nozzle through which the BR5.12 sample flows. This configuration permits the simultaneous measurement of the nonresonant background from water,[27] and the CARS signal from BR5.12 thereby minimizing the effects of any variability in the spectral intensities of the laser pulses. The two sets of probe laser pulses required for the CARS measurements are produced by amplitude division with a pellicle beam splitter. Each pair of probe laser pulses is focused separately into the reference and sample compartments using the same microscope objective (f = 5 cm). The angle between the laser beams is selected to ensure that the horizontal separation of the focal regions is about 0.8 mm. The signals from both compartments are collimated and focused onto the entrance slit of a triple monochromator (Spex, Triplemate). The wavelength-dispersed CARS signals are focused onto two separate, parallel stripes of a liquid-nitrogen cooled, CCD multichannel array (Princeton Instruments LN/CCD-1024-F/1 UV). The spectral resolution of these CARS measurements, determined primarily by the bandwidth of the ω_1 laser (*vide infra*), is <2 cm^{-1}.

The BR5.12 photoreaction is initiated via optical excitation (570 nm, <3 ps laser pulse, 3.0 nJ/pulse). The probe laser wavelengths (ω_1 = 663 nm and ω_s = 690−740 nm) are selected to generate preresonance CARS from BR5.12 and resonance CARS from T5.12. The energy of the probe laser pulses is set to 1.0 and 2.5 nJ for ω_1 and ω_s, respectively.[9]

The temporal synchronization of the laser pulses, monitored throughout the CARS experiment with an autocorrelator (FR-103XL, Femtochrome Research, Inc.) is characterized by a cross-correlation time (CCT) of ~8 ps for the two probe laser pulses. The temporal pulse widths for ω_1 and ω_s are 5.5 and 7 ps, respectively (assuming Gaussian pulse envelopes). The timing jitter between the excitation pulse (ω_p) and the two probe pulses (ω_1 and ω_s) is measured to be <2 ps, while the corresponding CCT (ω_p and ω_1) is 6.5 ps.

The timing sequences and delays between the three dye laser pulses are selected by three separate, but correlated optical delay lines designed for the picosecond time scale. Since T5.12 appears in <3 ps and decays within 18 ps, a delay sequence is chosen for recording the PTR/CARS data from T5.12 presented here. Procedurally, CARS spectra from BR5.12 (i.e., picosecond resonance CARS or PR/CARS) are recorded first while the PTR/CARS data from T5.12 are subsequently recorded for specific time delays between the pumping pulse (ω_p) and the two probing CARS pulses (ω_1 and ω_s).

(24) Brack, T. L.; Delaney, J. K.; Atkinson, G. H.; Albeck, A.; Sheves, M.; Ottolenghi, M. *Biophys. J.* **1993**, *65*, 964−972.

(25) Jäger, F.; Ujj, L.; Atkinson, G. H.; Sheves, M.; Livnah, N.; Ottolenghi, M. *J. Phys. Chem.* **1996**, *100*, 12066−12075.

(26) Ujj, L.; Jäger, F.; Atkinson, G. H. *Biophys. J.* **1998**, *74*, 1492−1501.

(27) Ujj, L.; Volodin, B. L.; Popp, A.; Delaney, J. K.; Atkinson, G. H. *Chem. Phys.* **1994**, *182*, 291−311.

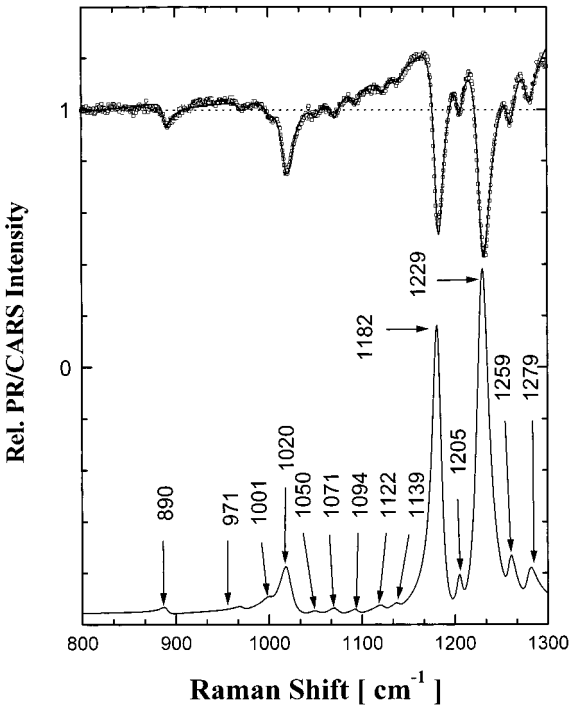

Figure 2. PR/CARS spectrum of BR5.12 in the 800 to 1300 cm^{-1} region. The nonresonant CARS signal from water only, indicated by the horizontal dashed line, is used to normalize the PR/CARS signal. The $\chi^{(3)}$-fit function is shown as a solid line overlapping the PR/CARS data (□). The corresponding background-free (Lorentzian line shapes) vibrational spectrum of BR5.12 derived from the $\chi^{(3)}$-fit is shown at the bottom. The wavenumber positions of selected bands are also presented.

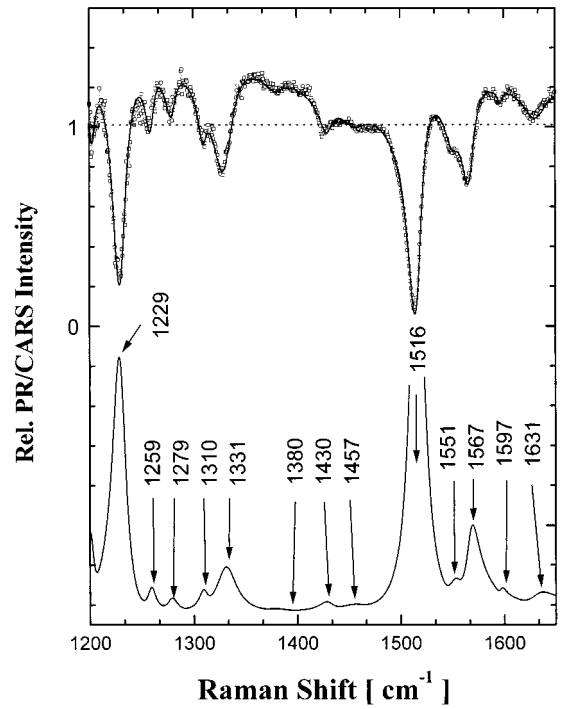

Figure 3. PR/CARS spectrum of BR5.12 in the 1200 to 1650 cm^{-1} region. The nonresonant CARS signal from water only, indicated by the horizontal dashed line, is used to normalize the PR/CARS signal. The $\chi^{(3)}$-fit function is shown as a solid line overlapping the PR/CARS data (□). The corresponding background-free (Lorentzian line shapes) vibrational spectrum of BR5.12 derived from the $\chi^{(3)}$-fit is shown at the bottom. The wavenumber positions of selected bands are also presented.

Table 1. Vibrational Band Parameters Derived from the $\chi^{(3)}$ Analysis of PR/CARS and PTR/CARS Spectra Recorded from BR5.12 and T5.12

BR5.12 RR[a] band max (cm^{-1})	BR5.12 PR/CARS[b] $\chi^{(3)}$ fit parameters[d] Ω_k (cm^{-1})	Γ_k (cm^{-1})	A_k	T5.12 PTR/CARS[c] $\chi^{(3)}$ fit parameters[d] Ω_k (cm^{-1})	Γ_k (cm^{-1})	A_k
				863	15	0.2
	890	5	0.1	880	4	0.08
	971	5	0.04	973	16	0.23
1008	1001	6	0.05	1001	6	0.05
	1020	8	0.35	1027 ± 2	8	0.08
	1050	6	0.06	1051	7	0.07
	1071	6	0.98	1075	6	0.02
	1094	4.5	0.07	1091	4.5	0.06
	1122	6	0.06	1124	13.5	0.17
	1139	5	0.04	1144	7	0.25
1177	1182	6	0.89	1186	9.5	0.63
	1205	4	0.18	1205	4	0.14
1221	1229	8	1	1229	8	1
	1259	5	0.18	1259	5	0.1
	1279	6	0.17	1279	6	0.07
1306	1310	5	0.15	1310	4	0.15
1327	1331	12	0.4	1331	13	0.44
	1380	11	0.05	1376	12	0.07
	1430	8	0.12	1432	12	0.19
	1457	18	0.09	1460	20	0.18
1514	1516	8	1.32	1520	10	1.4
	1551	8	0.15	1545	8	0.12
	1567	7.5	0.4	1567	14	0.55
	1597	3	0.05	1601	13	0.09
	1631	13	0.12	1629 ± 1.5	10	0.12

[a] Data from resonance Raman (RR) spectra.[23] [b] Data from picosecond resonance coherent anti-Stokes Raman spectra (PR/CARS, this work). [c] Data from picosecond time-resolved coherent anti-Stokes Raman spectra (PTR/CARS, this work). [d] Parameters (Ω_k-band origin, Γ_k-bandwidth (HWHM), and A_k-amplitudes) obtained from the $\chi^{(3)}$-fits of CARS spectra (800 to 1650 cm^{-1}) recorded from BR5.12 (Figures 2 and 3) and T5.12 (Figures 4 and 5). The amplitudes are normalized to that of the 1229-cm^{-1} band.

Results

A. PR/CARS Spectrum of BR5.12. The vibrational spectrum of ground-state BR5.12 reflects the initial chromophoric structure from which its photoreaction begins and, therefore, is the starting point for any vibrational analysis of the T5.12 intermediate. The S/N in the spontaneous resonance Raman data (900−1700 cm^{-1} region) for BR5.12 reported earlier[23] limited the observable features to only the six major bands (at 1514, 1327, 1306, 1221, 1177, and 1008 cm^{-1}). The significantly higher S/N of the PR/CARS data from BR5.12 (800−1650 cm^{-1} region) presented in Figures 2 and 3 makes it possible to observe at least 24 distinct vibrational features. These latter PR/CARS data, together with the respective $\chi^{(3)}$ fits, are shown at the top of each figure while the resultant vibrational spectra obtained by removing the nonresonant background signal and incorporating Lorentzian line shapes[26] are presented at the bottom of each figure. The positions of these CARS features are compared with RR data measured previously and are presented in Table 1.

B. PTR/CARS Spectrum of T5.12. Since PTR/CARS spectra are recorded from the mixture of BR5.12 and T5.12 present in the photoreaction at selected time delays after BR5.12 excitation, the relative contribution of BR5.12 must be quantitatively considered in the $\chi^{(3)}$ analysis before a CARS spectrum of T5.12 alone is obtained. The relative amount of BR5.12 present at each time delay can be determined from two independent measurements: (i) PTA data recorded from the same BR5.12 sample examined by PTR/CARS and (ii) vibrational band analysis of PTR/CARS spectra. Since the PTR/

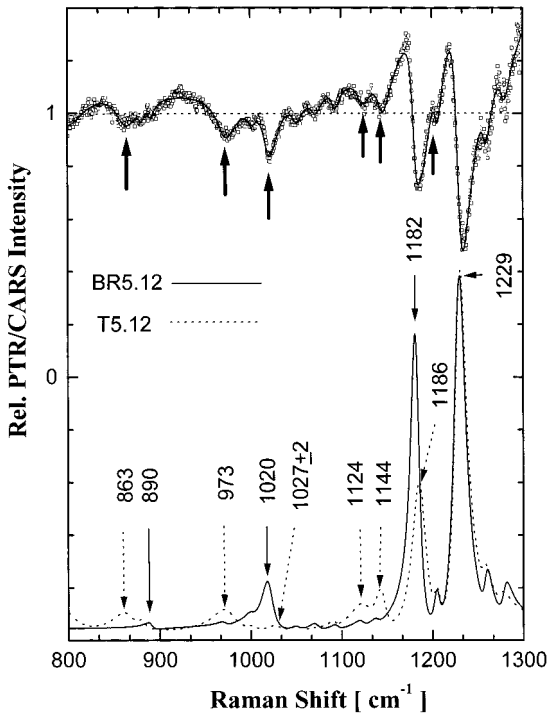

Figure 4. PTR/CARS spectrum indicating the presence of the T5.12 intermediate recorded 5 ps after 3-ps, 575-nm excitation of BR5.12 in the 800 to 1300 cm^{-1} region. The nonresonant CARS signal from water only, indicated by the horizontal dashed line, is used to normalize the PTR/CARS signal. The $\chi^{(3)}$-fit function is shown as a solid line overlapping the PTR/CARS data (□). The "↑" indicates the prominent changes in the 5-ps PTR/CARS spectrum. The corresponding background-free (Lorentzian line shapes) vibrational spectra of BR5.12 (solid line) and T5.12 (dashed line) derived from the $\chi^{(3)}$-fit are shown at the bottom. The wavenumber positions of selected bands are also presented.

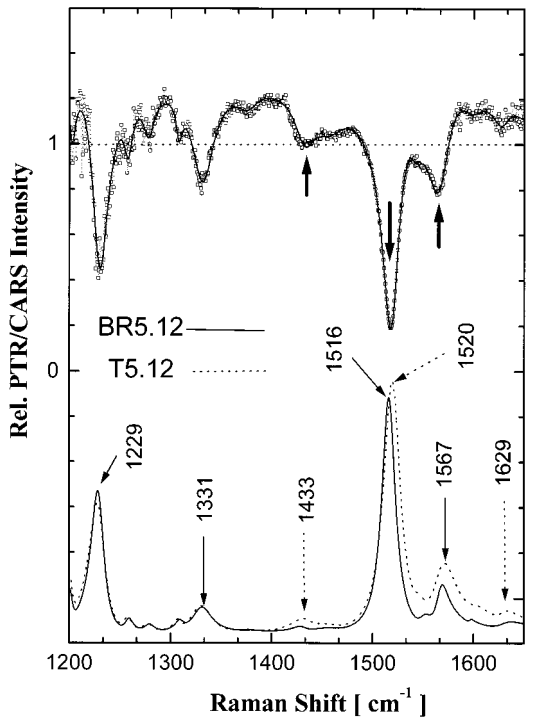

Figure 5. PTR/CARS spectrum indicating the presence of the T5.12 intermediate recorded 5 ps after 3-ps, 575-nm excitation of BR5.12 in the 1200 to 1650 cm^{-1} region. The nonresonant CARS signal from water only, indicated by the horizontal dashed line, is used to normalize the PTR/CARS signal. The $\chi^{(3)}$-fit function is shown as a solid line overlapping the PTR/CARS data (□). The "↑" indicates the prominent changes in the 5-ps PTR/CARS spectrum. The corresponding background-free (Lorentzian line shapes) vibrational spectra of BR5.12 (solid line) and T5.12 (dashed line) derived from the $\chi^{(3)}$-fit are shown at the bottom. The wavenumber positions of selected bands are also presented.

CARS spectrum recorded 5 ps after 570 nm excitation of BR5.12 (Figure 6) contains the largest contribution from T5.12, it is the focus of the quantitative analysis.

1. PTA data monitored at 663 nm (not presented) show that about 40% of the BR5.12 sample is optically converted into the excited electronic state by the 570-nm excitation (3 nJ/pulse) used here. A kinetic analysis of relative T5.12 concentration, based on its formation and decay rate constants,[15] BR5.12 absorption coefficient, and the CCT and energies of laser pulses, provides an estimate of the T5.12 contribution to the PTR/CARS spectrum at each time delay. These PTA data show that T5.12 contributes approximately 40% to the 5-ps PTR/CARS spectrum.

2. The time evolution of the CARS features assignable to BR5.12 into those assignable only to T5.12 can be viewed directly from PTR/CARS spectra recorded at selected time delays over the initial 50 ps of the BR5.12 photoreaction. Vibrational features assignable to T5.12 are observed to appear and disappear only as a function of reaction time, thereby reflecting the formation of T5.12 and its decay back to BR5.12.

The 5-ps PTR/CARS spectrum (Figure 6) contains a strong band at 1186 cm^{-1} (near 1182 cm^{-1} in the derivative PTR/CARS) and three smaller features at 863, 973, and 1144 cm^{-1}. All of these features decay to zero in the 10- and 50-ps PTR/CARS spectra (Figure 6). There is essentially no change in the 1229-cm^{-1} band (Figure 6). A significant change is observed when the 1516-cm^{-1} band of BR5.12 shifts to 1520 cm^{-1} (Figure 7). This 4-cm^{-1} shift is especially clear when PTR/CARS spectra recorded at 5 (large T5.12 concentration), 10, and 50 ps (only BR5.12 present) are compared. The intensity

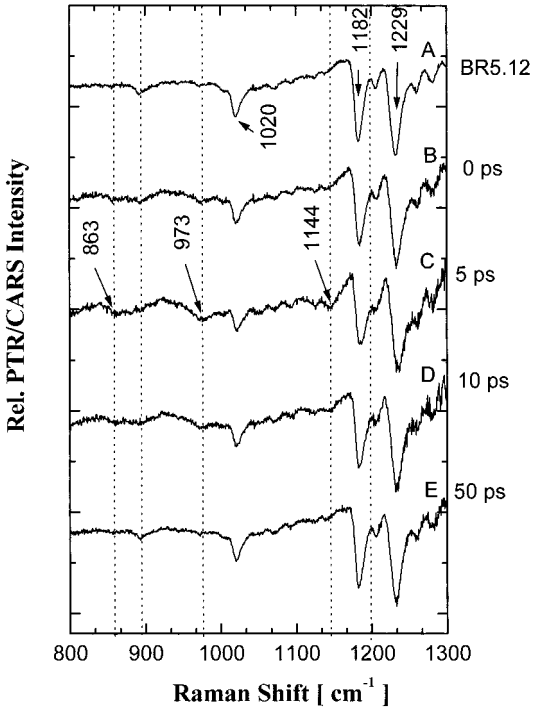

Figure 6. PR/CARS spectrum (800 to 1300 cm^{-1}) of BR5.12 in water (top) and PTR/CARS spectra of T5.12 and BR5.12 mixtures recorded at 0- (6-ps CCT), 5-, 10-, and 50-ps time delays (following 3-ps, 575-nm excitation of BR5.12). The vertical dashed lines indicate the most prominent, time-dependent spectral changes.

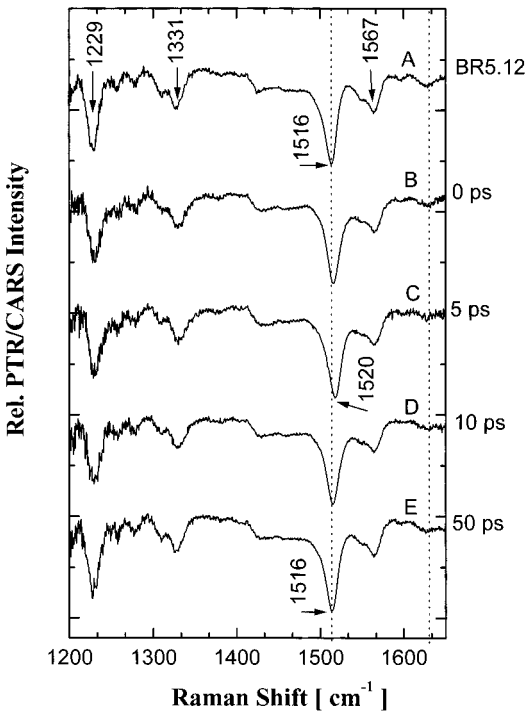

Figure 7. PR/CARS spectrum (1200 to 1650 cm^{-1}) of BR5.12 in water (top) and PTR/CARS spectra of T5.12 and BR5.12 mixtures recorded at 0- (6-ps CCT), 5-, 10-, and 50-ps time delays (following 3-ps, 575-nm excitation of BR5.12). The vertical dashed lines indicate the most prominent, time-dependent spectral changes.

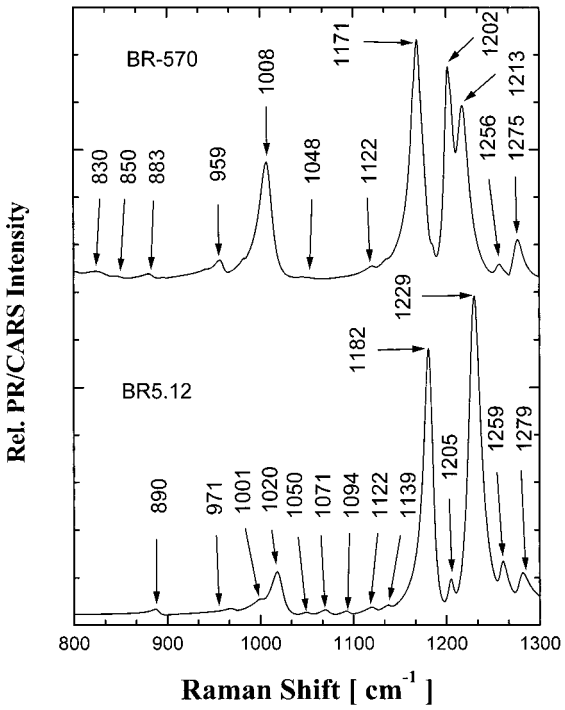

Figure 8. Background-free (Lorentzian line shape) vibrational spectra of BR-570 (upper) and BR5.12 (lower) in the 800 to 1300 cm^{-1} region.

of the 1567-cm^{-1} band also increases, but it is difficult to discern this change directly from PTR/CARS data. In all of these cases, band changes are readily resolved in the Lorentzian CARS spectra obtained after $\chi^{(3)}$ analysis.

This analysis of PTR/CARS vibrational spectra leads to the conclusion that T5.12 contributes about 40% to the 5-ps PTR/CARS data, clearly in good agreement with the PTA measurements, *vide supra*.

The resultant CARS spectrum of T5.12 together with the respective $\chi^{(3)}$ fits are presented for two overlapping spectral regions at the top of Figures 4 and 5. The corresponding vibrational spectra obtained by removing the nonresonant background signal and incorporating Lorentzian line shapes ($\chi^{(3)}$ fit) are presented at the bottom of each of these figures. The band maxima positions, bandwidths, and relative amplitudes are shown in Table 1.

Discussion

A. Spectra of Native BR-570 and BR5.12. The assignment of the degrees of freedom in BR5.12 to vibrational modes can be determined from comparisons with the analogous normal modes assignments for native BR-570. Initially, this comparison requires the identification of those normal modes in BR-570 perturbed by the incorporation of the five-membered ring found in BR5.12. Such vibrational assignments are especially effective for those vibrational modes where the major vibrational character of the normal mode is localized to a specific molecular bond (e.g., C−C stretch) or results in a distinct motion of a small number of nuclei grouped together (e.g., HOOP modes). Generally, the five-membered ring can be anticipated to cause minor perturbations to those BR-570 normal modes localized near the β-ionone ring and to cause major perturbations (e.g., create new normal modes) where the ring is directly involved in nuclear displacements.

The assignment of those vibrational modes anticipated to be perturbed by the ring can be derived partially from the assignments of vibrational modes in isotopic derivatives of native BR-570. Since the five-membered ring in BR5.12 spans the retinal between C_{12} and C_{14}, the effect of the ring on the polyene chain can be approximated by isotopically substituting the C_{12} and C_{14} positions. Vibrational assignments of the Raman spectra from the BR derivative containing $C_{12}D$ and $C_{14}D$ (BR-570/$C_{12}D$,$C_{14}D$) are available.[28] If those vibrational bands assigned to modes directly involved with $C_{12}D$ and $C_{14}D$ motions are excluded, the BR-570/$C_{12}D$,$C_{14}D$, and BR5.12 Raman spectra are remarkably similar (*vide infra*).

Totally, 24 vibrational bands assignable to BR5.12 can be identified in the PR/CARS spectra shown in Figures 8 and 9. The background-free PR/CARS spectra of BR-570 containing Lorentzian band shapes in the 800−1650 cm^{-1} spectral region are also presented in Figures 8 and 9 (top) to facilitate comparisons with BR5.12 (bottom) spectra.

1. HOOP and C−CH_3 Rocking Modes. The number of HOOP bands appearing in the BR5.12 spectrum is significantly smaller than those found for BR-570 (Figure 8), an observation attributed to the presence of the five-membered ring. Specifically, in BR5.12 (i) the hydrogen atoms at the C_{12} and C_{14} positions are absent and (ii) the retinal structure near C_{10} and C_{11} is forced into an approximately planar geometry. It is unlikely that the C−H bond geometry near C_7 and C_8 is altered by the ring.

a. The highest intensity BR-570 band(s) in this spectral region (883 cm^{-1}) is assigned to hydrogen wagging motions at respectively, C_{11}, C_{12}, and C_{14}.[29] Low-intensity bands at 889 and 1002 cm^{-1} are assigned to the C_7−C_8 hydrogen wag and the C_{15} wag, respectively.[28]

b. The relatively intense 890-cm^{-1} band of BR5.12 can be characterized in terms of $C_{10}H$ or $C_{11}H$ wagging and HC_7−

(28) Smith, S. O. Ph.D. Dissertation, 1985, pp 1−344.

(29) Smith, S. O.; Braiman, M.; Myers, A. B.; Pardoen, J. A.; Courtin, J. M.; Winkel, C.; Lugtenburg, J.; Mathies, R. A. *J. Am. Chem. Soc.* **1987**, *109*, 3108−3125.

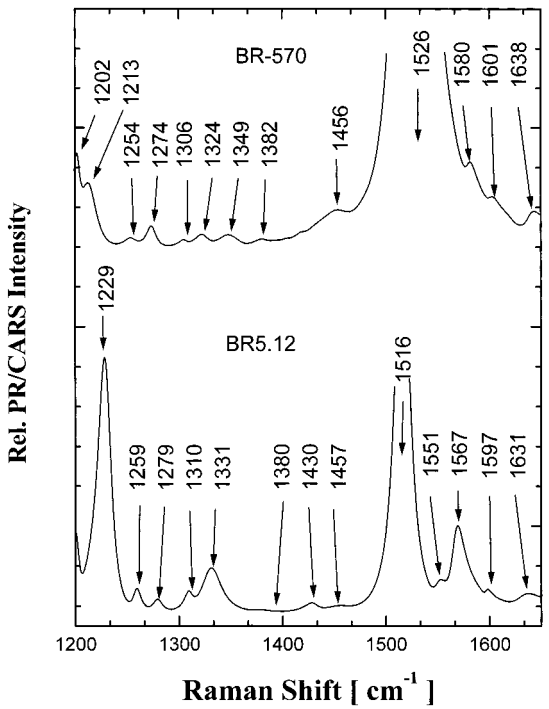

Figure 9. Background-free (Lorentzian line shape) vibrational spectra of BR-570 (upper) and BR5.12 (lower) in the 1200 to 1650 cm^{-1} region.

C_8H HOOP vibrations. Since no analogous band is observed in the BR-570($C_{12}D$,$C_{14}D$) spectrum,[28] the $C_{10}H$ and $C_{11}H$ wagging vibrations appear to make the major contribution to the 890-cm^{-1} BR5.12 band.

c. Since the weaker 971-cm^{-1} band of BR5.12 has counterparts in both the BR-570 and BR-570($C_{12}D$,$C_{14}D$) spectra,[28] it can be tentatively assigned to the analogous HC_7-C_8H HOOP mode.

d. The 1001-cm^{-1} band can be assigned from these PR/CARS data to the $C_{15}H$ wagging mode.[29] Analogous bands at almost the same position are found in the BR-570 and BR-570-($C_{12}D$,$C_{14}D$) spectra.[28]

The most intense $C-CH_3$ rocking vibration in BR-570, at 1008-cm^{-1}, contains primarily symmetric, in-plane rocking modes involving the methyl groups located at C_{19} and C_{20}.[29] The asymmetric combination of these modes in BR-570 is assigned to a low-intensity band at 1022 cm^{-1}. The $C-CH_3$ rocking mode in BR-570($C_{12}D$,$C_{14}D$) appears at essentially (±1 cm^{-1}) the same position as that found in BR-570.

Since the $C-CH_3$ rocking mode at C_{20} must be altered by the ring in BR5.12 (Figure 1), the absence of the 1008-cm^{-1} band in BR5.12 can be associated with the related reduction of symmetry. The 11-cm^{-1} frequency increase observed in BR5.12 can be attributed in general terms to the weak asymmetric coupling of the in-plane and out-of-plane motions (*vide supra*), a more detailed understanding of which can be obtained from the resonance Raman (RR) spectra of the artificial BR containing CD_3 at either C_{20} or C_{19}.[28] Specifically, perdeuteration of these methyl groups decouples the in-plane and out-of-plane methyl rocking modes, thereby causing the band assignable to the mode unaffected by deuteration to increase frequency by 10 cm^{-1}.[28] Since the methyl rocking coordinates couple only weakly, the 1020-cm^{-1} band in BR5.12 can be tentatively assigned to a single methyl rocking mode in which the major character originates with the C_{19} methyl group.

The weak 1048-cm^{-1} band of BR-570, assignable to an out-of-plane methyl rocking vibration (i.e., at the C_{19} position), can be associated with the same mode in BR5.12 having bands appearing at 1050 cm^{-1} and at 1047 cm^{-1} in BR-570-($C_{12}D$,$C_{14}D$).[28] The same assignment can be made for the 1050-cm^{-1} band in BR5.12.

The bands observed at 1380, 1430, and 1457 cm^{-1} are assigned to the symmetric deformations of the methyl groups. Since the 1457- and 1380-cm^{-1} bands in BR5.12 have the counterparts in the spectra of both BR-570 and BR-570-($C_{12}D$,$C_{14}D$), they are assigned to the $C_{19}-CH_3$ rocking mode. The frequency decrease of the 1442-cm^{-1} band in BR-570 to 1430 cm^{-1} in BR5.12 suggests that the 1430-cm^{-1} be assigned primarily to the $C_{20}-CH_3$ rocking mode.

The BR5.12 vibrational bands at 1071, 1122, and 1139 cm^{-1} have counterparts in the BR-570 spectrum appearing at approximately (±2 cm^{-1}) the same origin positions. These bands are associated with the β-ionone ring.

2. C−C Stretching Modes. The patterns of vibrational bands in the fingerprint region are significantly different in the native BR-570 and BR5.12 spectra (Figures 8 and 9). These fingerprint bands are primarily identified with C−C stretching modes which are strongly coupled to C−C−H rocking modes. By contrast, the fingerprint spectral region in BR5.12 is similar to that observed in BR-570($C_{12}D$,$C_{14}D$). Table 2 summarizes the C−C stretching vibrations of the chromophores in these three samples.

The 1216-cm^{-1} band in BR-570 contains C_8-C_9 stretching character which is coupled to the $C_{10}H$ and $C_{12}H$ rocking motions.[29] This same mode is assignable to the 1224-cm^{-1} band in the RR spectrum of BR-570($C_{12}D$,$C_{14}D$). By analogy, the intense 1229-cm^{-1} band in BR5.12 can be assigned to the C_8-C_9 stretching vibration.

The most intense BR-570 band in this spectral region appears at 1201 cm^{-1} and is assigned to the $C_{14}-C_{15}$ stretching mode which is coupled to the $C_{11}-C_{12}H$ bending mode. The analogous BR-570($C_{12}D$,$C_{14}D$) band at 1193 cm^{-1} can also be assigned to the $C_{14}-C_{15}$ stretching vibration. Such comparisons lead to the assignment of the intense 1182-cm^{-1} band in BR5.12 to the $C_{14}-C_{15}$ stretching vibration. The 19-cm^{-1} frequency decrease observed in BR5.12 can be attributed to a change in coupling between the C−C stretching vibrations and $C_{11}-C_{12}-H$ rock and alterations in the bond order (i.e., electron delocalization) in the polyene chain caused by the five-membered ring.

The 1171(±1)-cm^{-1} band in BR-570 contains mainly $C_{10}-C_{11}$ stretching character with some coupling to the $C_{11}-C_{12}-H$ and $C_{12}-C_{11}-H$ rocking motions. The analogous band appears as only a very weak shoulder in the RR spectrum of BR-570-($C_{12}D$,$C_{14}D$) and at a frequency position increased by 2−4 cm^{-1}. No analogous band of similar intensity is present in the PR/CARS spectrum of BR5.12 although the low-intensity 1205-cm^{-1} band is a reasonable candidate for the $C_{10}-C_{11}$ stretching vibration.

3. C═C Stretching Modes. The vibrational band patterns in the C═C stretching and Schiff-base region are substantially different for BR-570 and BR5.12 (Figure 9). The most intense BR-570 band at 1526(±1) cm^{-1}, assigned to the $C_7=C_8$, $C_{11}=C_{12}$, and $C_{13}=C_{14}$ stretching modes (with weak coupling to C−C stretching and HOOP modes), changes to 1516 cm^{-1} in BR5.12. The less intense bands, appearing as shoulders at 1580 and 1601 cm^{-1} in BR-570 and assigned to the $C_9=C_{10}$ and $C_{13}=C_{14}$ antisymmetric vibrations with a small contribution from the $C_5=C_6$ stretching mode, appear as three bands at 1551, 1567, and 1597 cm^{-1} in BR5.12, with the intensity of the 1567-cm^{-1} band being the largest (Figure 9). By analogy, therefore, the 1516-cm^{-1} band in BR5.12 can be assigned to the $C_{11}=C_{12}$ and $C_{13}=$

Table 2. Positions and Major Characteristics of the Band Assignments of the C−C Stretching Vibrations in RR and PR/CARS Spectra Recorded from BR-570, BR-570($C_{12}D$,$C_{14}D$), and BR5.12

BR-570		BR-570($C_{12}D$,$C_{14}D$)		BR5.12	
resonance Raman band max[a] (cm^{-1})	assignment	resonance Raman band max[b] (cm^{-1})	assignment	PR/CARS band origin[c] (cm^{-1})	assignment
1170(2) intense	$C_{10}-C_{11}$ stretch	1176 weak	$C_{10}-C_{11}$ stretch	1205 weak	$C_{10}-C_{11}$ stretch
1201 intense	$C_{14}-C_{15}$ stretch	1193 intense	$C_{14}-C_{15}$ stretch	1182 intense	$C_{14}-C_{15}$ stretch
1216 intense	C_8-C_9 stretch	1224 intense	C_8-C_9 stretch	1229 intense	C_8-C_9 stretch

[a] Taken from refs 28 and 29. [b] Taken from ref 28. [c] Picosecond resonance coherent anti-Stokes Raman spectra (this work).

C_{14} stretching vibrations while the 1567-cm^{-1} band in BR5.12 can be assigned to the $C_{13}=C_{14}$ and $C_9=C_{10}$ stretching modes.

These assignments of the C=C stretching modes are supported by the vibrational bands found in BR-570($C_{12}D$,$C_{14}D$): the most intense band at 1509 cm^{-1} is assigned to the $C_{11}=C_{12}$ and $C_{13}=C_{14}$ in-phase stretching vibrations while the band at 1574 cm^{-1} is assigned to the out-of-plane combination of the $C_{13}=C_{14}$ and $C_9=C_{10}$ stretching modes.[28] Furthermore, two low-intensity bands appear in the RR spectra of two different, monodeuterated BR samples: at 1545 cm^{-1} in BR-570($C_{12}D$) and at 1543 cm^{-1} in BR-570($C_{14}D$).[28] The absence of any analogous band in the RR spectrum of BR-570($C_{12}D$,$C_{14}D$) indicates that the local symmetry of these normal modes is broken by deuterium substitution respectively at C_{12} and C_{14}. Since the same type of symmetry breaking occurs in BR5.12, the corresponding 1551-cm^{-1} band can also be assigned to the same modes as there are in BR-570($C_{12}D$) and BR-570($C_{14}D$).[28]

The BR5.12 band observed at 1597 cm^{-1} is assigned to the $C_7=C_8$ and $C_5=C_6$ stretching modes. This assignment is supported by the appearance of analogous bands at essentially the same positions in all of the deuterated derivatives of BR described here: at 1601 cm^{-1} in BR-570, at 1600 cm^{-1} in BR-570($C_{12}D$,$C_{14}D$), at 1598 cm^{-1} in BR-570($C_{12}D$), and at 1598 cm^{-1} in BR-570 ($C_{14}D$).[28]

4. Schiff-Base Modes. The band at 1638 cm^{-1} in BR-570 is assigned to the C=N stretching mode associated with the protonation state of the Schiff-base and its lysine linkage to the opsin. The frequency of this band decreases by about 15 cm^{-1} in deuterated BR samples. The 1631-cm^{-1} band in BR5.12 also can be assigned to the C=N stretching, Schiff-base mode. In general, these BR-570 and BR5.12 bands are similar indicating that the respective Schiff-base bonding environments are also similar. This means that the role(s) of any water molecules and/or amino acids in hydrogen bonding at the Schiff-base remain largely unchanged between BR-570 and BR5.12. There is no indication that water molecules and/or retinal−amino acid interactions are significantly altered by introducing the five-membered ring.

The 1349-cm^{-1} band in BR-570, assigned to the NH in-plane rocking mode, decreases to 1331 cm^{-1} in BR5.12, indicating that some changes along the retinal backbone bonding are found in BR5.12 (as anticipated when the ring is added).

B. Spectra of BR5.12 and T5.12. The appearance of distinct vibrational bands in the spectra of the optically excited, BR5.12 sample, in addition to those of ground-state BR5.12, shows that T5.12 is a stable intermediate with well-defined vibrational modes and that the molecular structure of the retinal chromophore within T5.12 is distinct from that in BR5.12. A detailed understanding of the structure changes occurring in the BR5.12 photoreaction can be derived from a vibrational analysis of the T5.12 PTR/CARS spectrum.

1. HOOP and CH_3 Rocking Modes. The relatively strong intensities of the 863- and 973-cm^{-1} HOOP bands in the CARS spectrum of T5.12 indicate that the polyene chain contains a

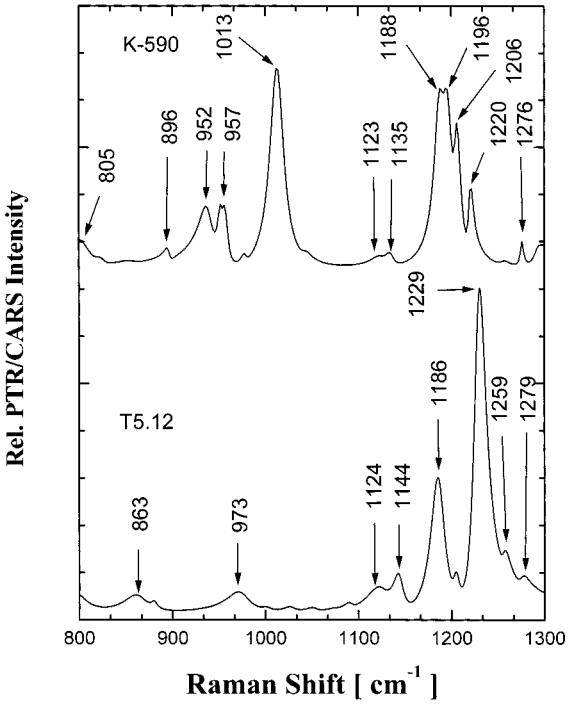

Figure 10. Background-free (Lorentzian line shape) vibrational spectra of K-590 (upper) and T5.12 (lower) in the 800 to 1300 cm^{-1} region.

significant amount of out-of-plane motions and may be twisted, thereby resulting in enhanced polarizability changes at specific bonds. This polyene backbone twisting disappears when BR5.12 is reformed from T5.12 on the (18 ± 1)-ps time scale.[23] The assignment of the 973-cm^{-1} band to the $HC_7=C_8H$ HOOP mode is based on the assignment of the BR5.12 band at 971 cm^{-1}, *vide supra*. The significantly greater intensity of the T5.12 band indicates that it is twisted around the $C_7=C_8$ bond. The other main HOOP band in T5.12, at 863 cm^{-1}, can contain contributions from the C_7-H, C_8-H, $C_{11}-H$, and $C_{10}-H$ out-of-plane local modes. The relationship between the HOOP band intensities and the degree of twisting at specific, localized C=C−C bonds has been well established from both Raman and IR studies.[30−32]

The most dramatic change occurs in the CH_3 rocking modes. The 1020-cm^{-1} band in BR5.12 is essentially absent in the vibrational spectrum of T5.12 (Figure 10). This mode is remarkably stable in all the vibrational spectra of the BR-570 intermediates measured to date, regardless of the conformation of the chromophore in the protein binding pocket.[28] These changes in T5.12 indicate that the $C_{19}-CH_3$ methyl group

(30) Deng, H.; Manor, D.; Weng, G.; Rath, P.; Koutalos, Y.; Ebrey, T.; Gebhard, R.; Lugtenburg, J.; Tsuda, M.; Callender, R. H. *Biochemistry* **1991**, *30*, 4495−4502.

(31) Curry, B.; Broek, A.; Lugtenburg, J.; Mathies, R. A. *J. Am. Chem. Soc.* **1982**, *104*, 5274−5286.

(32) Eyring, G.; Curry, B.; Broek, A.; Lugtenburg, J.; Mathies, R. *Biochemistry* **1982**, *21*, 384−393.

interacts (e.g., through steric hindrance) with one or more of the amino acids in the binding pocket. In T5.12, the rocking motion of the C_{19} $-CH_3$ group apparently becomes blocked which simultaneously introduces strain in the polyene chain resulting in a twisting of the chromophore, *vide supra*.

2. C−C Stretching Modes. The changes in the fingerprint region indicate that the *all-trans* configuration of BR5.12 is preserved in T5.12. The BR5.12 band at 1182 cm^{-1}, assigned mainly to the $C_{14}-C_{15}$ stretching mode, increases to 1186 cm^{-1} in T5.12. The relative intensity change is comparable to that of the 1229-cm^{-1} band. The observed frequency shift can be explained by alterations near the $C_{13}=C_{14}$ bond in BR5.12, even in the presence of the relatively rigid, five-membered ring spanning the $C_{12}-C_{13}=C_{14}$ bonds.

3. C=C Stretching Modes. Because the vibrational pattern of bands in T5.12 assigned to the C=C stretching modes is the same as that found in BR5.12, the assignments are expected to be similar. Thus, the 1520-cm^{-1} band of T5.12 is assigned to the $C_{11}=C_{12}$ and $C_{13}=C_{14}$ stretching vibrations while the 1567-cm^{-1} band of T5.12 can be assigned primarily to the $C_{13}=C_{14}$ and $C_9=C_{10}$ stretching modes. The frequency shifts of the C=C bonds are related to the absorption band maxima positions in native BR-570 intermediates,[33] namely a frequency decrease of the most intense band correlates with a "red" shift of the absorption band. Because the position of the 1520-cm^{-1} band **increases** by 4 cm^{-1}, this relationship is apparently **not** valid for T5.12. This inconsistency could be interpreted in at least two ways. The absorption assigned to T5.12 could be from an electronic (e.g., excited) state other than that of ground-state BR5.12 in which case the entire degree of resonance delocalization of electron energy would be different. Alternatively, the position of the measured T5.12 absorption maximum may be shifted due to the simultaneous presence of stimulated emission (if T5.12 is an excited electronic state) and ground-state absorption. In both cases, the relationship between C=C stretching frequency and absorption maximum would be altered.

4. Schiff-Base Modes. The position of the BR5.12 band at 1567 cm^{-1} does not change in T5.12 (Figure 5), but it broadens by a factor of 2. The first observation indicates that the Schiff-base bonding environment (including the role of water molecules bound to the NH) is not significantly changed upon the formation of T5.12. Thus, movement of water molecules near the Schiff base is not consistent with these vibrational data. It is important to note that the vibrational (PTR/CARS) spectrum of K-590 contains essentially no bands in the Schiff-base region which is a substantial change from the strong 1638-cm^{-1} Schiff-base band observed in BR-570. These data show that the Schiff-base bonding environment in K-590 is significantly different than in BR-570 which is in contrast with that observed for T5.12 relative to BR5.12. The second observation may indicate faster dephasing times in T5.12 relative to BR5.12.

The absence of changes in the 1331- and (1629 ± 1.5)-cm^{-1} bands for T5.12 and in the 1631-cm^{-1} band of BR5.12 in T5.12 indicates that the Schiff-base linkage of the chromophore to the protein is the same in both BR5.12 and T5.12. These bands are assigned to the C=N stretching and the NH in-plane rocking modes, respectively.

C. Spectra of T5.12 and Native BR Intermediates. There are three native BR intermediates that might be considered for comparison with T5.12: K-590, J-625, and I-460. The identification of T5.12 with one of these intermediates may relate the reaction mechanism (coordinate) underlying the BR5.12/T5.12 transformation with that found in the native BR photocycle. Establishing the relationship of the T5.12 structure and those of J-625 and K-590 may improve an understanding of the retinal structural changes that comprise the reaction coordinate(s) in the native BR photocycle.

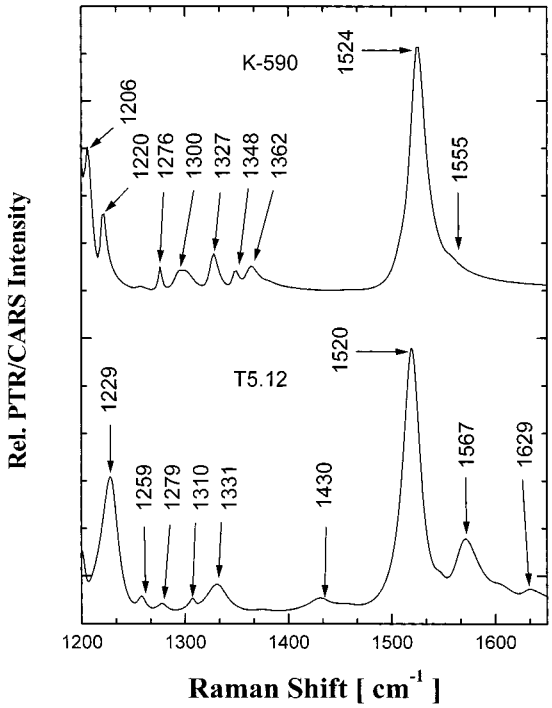

Figure 11. Background-free (Lorentzian line shape) vibrational spectra of K-590 (upper) and T5.12 (lower) in the 1200 to 1650 cm^{-1} region.

1. Spectra T5.12 and K-590. Recent PTR/CARS data demonstrate that the overall retinal structure of K-590 (13-*cis*) appears within 10 ps and remains unchanged for at least 100 ns. This result is consistent with a wide range of accumulated evidence suggesting that K-590 has a 13-*cis* retinal.[9,25,34−36] Some of the out-of-plane motion observed in the initial 100 ps of the K-590 lifetime diminishes within 4 ns to form a more planar 13-*cis* retinal structure[13] prior to its transformation into the L-550 intermediate over a microsecond time interval.[37] Thus, a comparison of the T5.12 and K-590 PTR/CARS spectra can establish whether T5.12 also contains a 13-*cis* or 13-*cis*-like retinal.

The background-free, Lorentzian line shape PTR/CARS spectra of K-590 (top) and T5.12 (bottom) over the 800−1650 cm^{-1} spectral region are shown in Figures 10 and 11.

a. HOOP and CH_3 Rocking Modes. The vibrational bands in the 800−1050-cm^{-1} region (HOOP and CH_3 rocking modes) observed for native K-590 and T5.12 are completely different in both position and relative intensities (Figures 10 and 11). Although the HOOP modes for T5.12 (863 and 973 cm^{-1}) show that its polyene chain is distorted to some degree relative to the retinal in BR5.12 (*vide supra*), the retinal in T5.12 is significantly less distorted than that in K-590 (805, 896, 952, and 957 cm^{-1}). The increased HOOP band intensities found in K-590 result from the strongly enhanced Raman scattering in these specific modes when the retinal is torsionally distorted. The

(33) Honig, B.; Ebrey, T.; Callender, R. H.; Dinur, U.; Ottolenghi, M. *Proc. Natl. Acad. Sci. U.S.A.* **1979**, *76*, 2503−2507.

(34) Lohrmann, R.; Grieger, I.; Stockburger, M. *J. Phys. Chem.* **1991**, *95*, 1993−2001.

(35) Smith, S. O.; Lugtenburg, J.; Mathies, R. A. *J. Membr. Biol.* **1985**, *85*, 95−109.

(36) Atkinson, G. H.; Brack, T. L.; Blanchard, D.; Rumbles, G. *Chem. Phys.* **1989**, *131*, 1−15.

(37) Váró, G.; Lanyi, J. K. *Biochemistry* **1991**, *30*, 5008−5015.

HOOP bands in the 940−990-cm^{-1} region are especially important since they have been assigned to out-of-plane modes involving the $C_{12}-C_{13}=C_{14}$ bonds.[28] Thus, the appearance of the 973-cm^{-1} band with even moderate intensity in the T5.12 spectrum (Figure 10) indicates that a modest degree of out-of-plane distortion around the $C_{12}-C_{13}=C_{14}$ bond occurs even in the presence of the five-membered ring. Overall, however, the type and degree of out-of-plane motion present in T5.12 is significantly smaller than that appearing in the highly distorted K-590.

The absence of a prominent CH_3 rocking mode in T5.12 (Figure 10) is especially important to note since it reflects a major difference in CH_3-C rocking modes relative to BR5.12. The moderately intense 1020-cm^{-1} band in the BR5.12 spectrum completely disappears when T5.12 is formed (Figure 4). Absence of a significant CH_3 rocking mode is also in contrast to the intense CH_3 rocking band at 1013 cm^{-1} in the K-590 spectrum (Figure 10). Thus, the CH_3 rocking modes in T5.12 and K-590 are different.

b. C−C Stretching Modes. The *trans*/*cis* isomerization at the $C_{13}=C_{14}$ bond that dominates the native BR photocycle, and, therefore, the structure of K-590, causes major changes in the C−C stretching modes which are reflected in the 1050−1300 cm^{-1} band region of the BR-570 and K-590 vibrational spectra (Figure 10): the BR-570 bands at 1172, 1205, 1216, and 1256 cm^{-1} shift to 1188, 1196, 1206, and 1220 cm^{-1} when K-590 is formed.[9,25,28] Thus, completely different band patterns can be associated with the *all-trans* and 13-*cis* configurations.

A comparison of PR/CARS spectra from BR-570 and BR5.12 (*vide supra*) demonstrates that the latter species has a significantly simpler C−C stretching bands pattern: at 1182 and 1229 cm^{-1}. Only the first band (assigned to the $C_{14}-C_{15}$ stretching mode) shifts to 1186 cm^{-1} upon T5.12 formation (Figure 4). Thus, the C−C stretching region in T5.12 contains only two bands, one of which (1229 cm^{-1}) has not changed from the position found in BR5.12.

The C−C stretching bands in T5.12, therefore, indicate that its retinal is not in a *cis* or *cis*-like configuration nor is its retinal backbone remotely close to the structure found in K-590.

c. C=C Stretching and Schiff-Base Nitrogen Modes. The C=C stretching modes in BR-570 also undergo major changes during *trans*/*cis* isomerization and, thus, the formation of K-590: The BR-570 band at 1526 cm^{-1} **decreases** to 1524 cm^{-1} and its intensity decreases a factor of 10 when K-590 is formed.[9] By contrast, the 1516-cm^{-1} band in BR5.12 **increases** to 1520 cm^{-1} when T5.12 is formed. Thus, the changes in the C=C stretching band positions are completely different for BR-570/K-590 and BR5.12/*T*5.12, the latter being twice as large and in the opposite direction energetically. The differences in the C=C stretching bands show that the T5.12 and K-590 structures are themselves distinct.

d. Summary. Collectively, the vibrational data from all three spectral regions show that T5.12 and K-590 have completely different vibrational structures. While K-590 has significant out-of-plane motion,[9] essentially no analogous out-of-plane distortion occurs when T5.12 is formed (Figures 4 and 10). There are no substantial changes in the C−C or C=C stretching modes that reflect isomerization of the retinal backbone in T5.12 which is in contrast to the changes (assigned to $C_{13}=C_{14}$ *trans* to *cis* isomerization) appearing in the K-590 spectrum.[9,13] Although the five-membered ring in BR5.12 effectively blocks *trans*/*cis* $C_{13}=C_{14}$ isomerization, some distortion (e.g., twisting) within the retinal does occur when T5.12 appears. At least some of this backbone twisting appears to involve the $C_{13}=C_{14}$ bond even though the transient flexibility of the five-membered ring is thought to be limited. Whatever the precise nature of the distortion, T5.12 relaxes back to the original retinal structure in BR5.12 within 20 ps. No stable 13-*cis*, K-like intermediate is formed.

The PTR/CARS spectrum of T5.12 is clearly different from that of K-590 demonstrating not only that T5.12 does not isomerize around the $C_{13}=C_{14}$ bond, but also that T5.12 does not isomerize around any of the other retinal bonds in BR5.12. These conclusions are consistent with those from previously published PTA results.[23]

2. T5.12 in Comparison with J-625 and I-460. The precise relationship(s) between T5.12 and either of the femto/picosecond, native BR intermediates, J-625 and I-460, remains unclear since much of the kinetic, spectroscopic, and structural characterization of the latter two intermediates also remains to be firmly established. Although some general comparisons can be made to support a particular analysis (e.g., the transient absorption spectra of T5.12 and J-625 both shift to the red of their respective ground-state absorptions), the basis for other comparisons remains unclear (e.g., the transient absorption spectrum of I-460 appears over an extremely wide spectral range extending to both the red and blue of the ground-state BR-570 absorption spectrum).[18,19] As J-625 and I-460 become more fully characterized, their respective relationship(s) to T5.12 can be more clearly established. Nonetheless, the PTR/CARS data presented here provide new insight into the evolution of the vibrational degrees of freedom, and thereby the structural changes, to be anticipated during the early stages of the BR photocycle represented by J-625 and I-460:

a. The frequency of the C=C stretching mode **increases** relative to ground-state BR-570 and subsequently **decreases** when 13-*cis* to all-trans isomerization occurs (e.g., when K-590 is formed).

b. The Schiff-base C=N−H mode remains unchanged indicating that its bonding environment is unchanged (i.e., any water bonding/position, protein interaction, and/or lysine configuration is the same as in the ground state).

c. The C−C stretching band pattern indicates a primarily *all-trans* retinal configuration although changes in the π-electron delocalization among these bonds alter their absolute frequencies.

d. The intensity of the CH_3 rocking mode decreases significantly, thereby indicating that the interaction between the retinal near the C_{19} and/or C_{20} bonds and the surrounding protein changes.

e. The intensities of the HOOP modes increase substantially indicating significant twisting/distortion of the retinal backbone.

The proposed changes in the retinal structure derived from the T5.12 data may be verified experimentally through PTR/CARS data (where feasible) from J-625 and/or I-460.

3. T5.12: Ground or Excited Electronic State. Although direct evidence determining whether T5.12 is a ground or excited electronic state is not derived from these PTR/CARS data, it is useful to note that the lifetime of T5.12, as measured via both PTA[23] (17 ± 1 ps) and PTR/CARS (18 ps) (this work) measurements, agrees well with the stimulated emission lifetime of BR5.12 (18 ps).[16] Such agreement supports the assignment of T5.12 as an excited electronic state, in which case the PTR/CARS data presented here are from an excited electronic state of the protein. The significance of whether T5.12 is an excited or ground electronic state with respect to the corresponding electronic properties of native J-625, however, cannot be drawn directly. The lifetimes of I-460 (200−500 fs) and J-625 (3.5

ps) are substantially different and neither fluorescence nor stimulated emission has been observed from J-265. The introduction of the five-membered ring to form BR5.12 may influence the electronic state properties of J-625, thereby distinguishing them from those of T5.12. What can be deduced from these PTR/CARS data, however, is that distinct structural changes in the retinal chromophore occur prior to C_{13}═C_{14} isomerization (structurally restricted in BR5.12) and that similar retinal structural changes should be anticipated in native J-625 if C_{13}═C_{14} isomerization is not the initial structural change in retinal to occur in the native BR photocycle (i.e., if J-625 remains *all-trans* rather than 13-*cis*).

Acknowledgment. This research is supported by a grant to G.H.A. from the National Institutes of Health (GM46439) and by grants to M.O. and M.S. L.U. wishes to gratefully acknowledge Innovative Lasers Corp. for financially supporting his work on this project.

JA991447E